Bima Journal of Science and Technology, Vol. 8(4B) Jan, 2025 ISSN: 2536-6041

DOI: 10.56892/bima.v8i4B.1201

Design and Implementation of a Backup Laptop Power Bank

L. Sa'adu[1],Y. Yusuf[2], Abdullahi I.[1*] and A. B. Isah[1]

[1]Department of Physics Federal University Gusau, Zamfara State, Nigeria
[2]Department of Physics Zamfara College of Arts & Science Gusau, Zamfara State, Nigeria

Corresponding Author's Email: sci00316@gmail.com

ABSTRACT

Power bank is any portable device design for charging electronic device like mobile phones or tablet computers while on the move. Boost converter also known as a step-up converter (SC) is a circuitry design aimed at stepping-up of applied DC input. SC is mostly used in applications where a higher voltage level is required, such as in solar panels and LED lightening. For instance, powering a 12-volt LED lamp using a 3.7-volt lithium ion battery. A power bank integrated with boost converter was designed and implemented with the aim of being used as an alternative means of powering a laptop. The power bank output was designed to be variable such that it can power variety of laptops irrespective of its input supply, a feature not available in the commercial power banks. The internal storage battery of the system used is lithium ion of potential difference (PD) 9.6 volt, while the output PD is targeted at the range of 9.6 to 20 volt. The storage battery and the boost converter circuit were to be protected by deep discharge and reverse polarity protection circuit. Moreover, the protection circuit can be bypassed while operating the system directly from solar panel. Prior to construction, Proteus software was used for design and simulation. The construction materials were obtained locally. Several laptops were used to test the system, and it was discovered to be functioning well.

Keywords: Power bank, Boost Converter, Potential Difference (PD), Proteus, Software

INTRODUCTION

Nowadays, the reliance on portable electronic devices such as smartphones, tablets, laptops, smartwatches, and even wireless earphones is rising exponentially, however; the key challenge is that of providing stable power supply on the go. Power banks (PB) have become essential in this regards due to their ability to provide power in times of need thereby maintaining connectivity, productivity, and conveniency (Czerniak et al., 2021; Kuncoro et al., 2023; Shukla et al., 2024). PB is any portable device design for charging electronic device like mobile phones or tablet computers while on the move. While most devices such as laptops require higher voltage (up to 20V in some cases) for charging, typical PB consists of one or more lithium-ion cell with a nominal voltage of approximately 3.7 V per cell (Akankpo *et al*., 2023). Thus, the main challenges are that the voltage supplied by the PB's battery is not enough to charge most laptops and other USB-powered devices, intermittency, and slow response (Almutairi *et al*., 2021). A boost converter on the other hand is a DC-to-DC converter that steps up applied potential difference to higher values by using carefully interconnected electronic components such as inductors, MOSFETs, diodes and capacitors (Sedaghati & Pourjafar, 2020). Thus, a strategic integration of boost converter into PBs design could results in a regulated and increased voltage suitable for charging laptops and other similar gadgets.

SC inputs typically have a constant or regulated voltage output and an uncontrolled voltage input. The two primary categories of regulators are switching and linear regulators.

DOI: 10.56892/bima.v8i4B.1201

A power transfer stage and control circuitry are features of all regulators that sense output PD thereby modifying the power transfer stage ensuring a steady output supply (Baby, 2015). As DC-DC converters, switching converters exhibits higher and noble efficiency compared with linear regulators (D'Amico *et al*., 2006). Output voltage of renewable energy systems or rectifier converter is basically unregulated DC voltage. A boost converter (BC) is a dc-dc converter that changes the low unregulated input voltage into higher and regulated output voltage, it is being integrated in the prominent 'Joule thief' circuit as PD increment instrument. The circuit is a topology utilized with reduced power battery uses, and is purposed at the capacity of a lift converter to 'take' the leftover energy in a battery (B. Yang, W. Li, Y. Zhao, 2010; Norum, 2010)The role of the DC-DC boost converter is to boost the photo voltaic (PV) source voltage in order to extract maximum power from the PV array. The SC is mostly used in applications where a higher voltage level is required, such as in solar panels and LED lightening (Ghavipanjeh Marangalu et al., 2021). The DC input is normally supplied by solar panels and therefore is fluctuating and uncontrolled, however, the corresponding DC output voltage must be regulated irrespective of the fluctuating nature of the input (Hasaneen & Mohammed, 2008).

In this paper, a power bank of variable output was design and constructed. The design differs from commercial PB by having two features, a variable output supply and deep discharge/reverse polarity, while that of the commercial is having a battery level indicator, although some were having two fixed output sources. Furthermore, it is designed to power variety of laptops of input PD ranging from 12 to 20 volt. Reverse polarity and deep discharge protections were added to the system design which may be bypassed while connecting it directly to the solar panel.

THEORY

Boost Converter

A boost converter is a circuit that increases value of the DC input giving out steady and stepped output voltage. This converter encompasses components such as diodes, transistors, and inductor coils. Capacitors are integrated in the design to cushion the possible rippling effect from the DC output as a result of switching action. Figure1 demonstrates the basic boost switching circuit. It usually works in two separate levels: when the switch is in the ON position, its contacts are closed, increasing the inductor current; when the switch is in the OFF position, it opens, providing the sole way for the coil's current to pass via the fly-back diode "D" and the side by side connection of the capacitor and load, thus, allowing the transfer of energy from the capacitor while it is turned on. Once the switch (S) is ON position (closed), the PD across the inductor (L) is $V_L = V_i - V_o$. The current flowing via the coil increases proportionately, since there is a diode connected in a reverse-biased the current cannot flow through. For OFF state (the switch is in the off position), the diode is forward biased, thus, the PD applied to the coil is given by is $V_L = - V_o$ (ignoring the voltage drop across diode) and the inductor current is reduced.

Bima Journal of Science and Technology, Vol. 8(4B) Jan, 2025 ISSN: 2536-6041

DOI: 10.56892/bima.v8i4B.1201

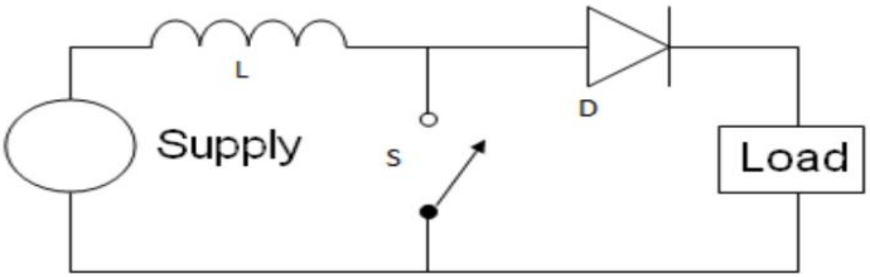

Figure 1: Basic Boost Circuit(Lopa et al., 2016)

Deep Discharge and Reverse Voltage Protection

Energy storage proved to be an important part of renewable energy applications. The main focus of the energy storage materials is on batteries. However, the lifespan of batteries is limited by the number of charge-discharge cycles they can endure. Degradation over time can reduce system efficiency and increase maintenance costs. Therefore, deployment of control techniques ensures optimal battery efficiency. In this regards, the constant-current constant-voltage technique is commonly used (Edison *et al*., 2018)

As the combination of photovoltaic and hybrid systems proliferate, solar batteries offer a unique energy storage solution for these systems to guarantee a supply of energy for users. Control and management techniques are crucial because of the sensitivity of solar batteries and the erratic functioning of photovoltaic systems that rely on solar radiation (Ezzitouni *et al*., 2021). Avoiding deep discharge or overcharging Li-Fe cells is necessary to guarantee their adequate lifespan and, occasionally, their operational safety. Manufacturers of batteries forbid such operations, and their datasheets don't explain how batteries behave in certain circumstances. (Prochazka *et al*., 2016)

MATERIALS AND METHODS

System Design

The basic system's block diagram is exhibited in Figure 2. The steps include reverse polarity protection circuit, oscillator, boost converter circuit, deep-charge control circuit and DC voltmeter module. The circuit design prepared and simulated in Proteus software. Table 1 presents the parameters of the boost converter.

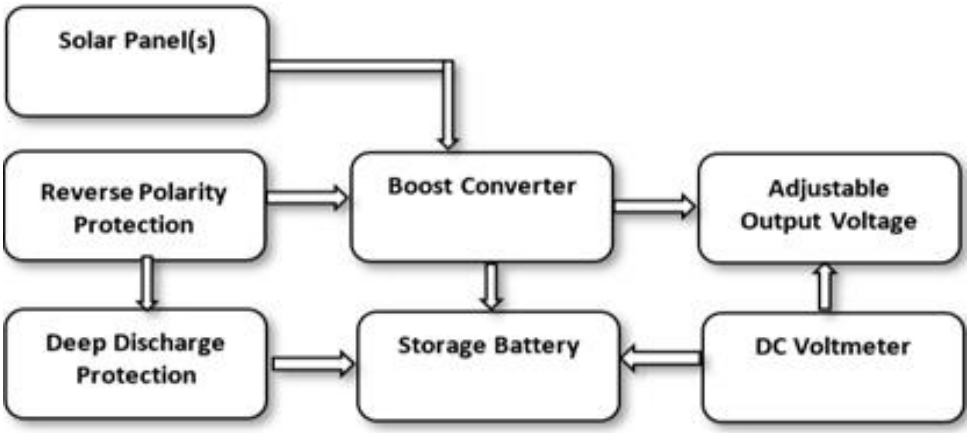

Figure 2: Block Diagram of the Design set up

Bima Journal of Science and Technology, Vol. 8(4B) Jan, 2025 ISSN: 2536-6041

DOI: 10.56892/bima.v8i4B.1201

Table 1: Design Parameters of the Proposed Converter

S/N	Variable	Symbol	Value
1	Input Voltage	*Vi*	9.6 Volt
2	Output Voltage	*Vo*	20 Volt
3	Output Power	*Po*	65 Watt
4	Switching Frequency	*Fs*	63.7 kHz
5	Output Voltage Ripple	$\Delta Vo\%$	1 %
6	Inductor Current Ripple	$\Delta I_L\%$	10%
7	Output Current	~~*Imax*~~	3.25 A

Converter Circuit Design

The basic power stage of a boost converter is shown in Figure 3. The switch is a MOSFET driven by an integrated circuit (IC). Parameters needed for power stage calculations are input voltage range Vin(min) and Vin(max), nominal output voltage (Vout), maximum output current (Iout) and power switch. The oscillator frequency chosen is 63.7 kHz. Standard resistor and capacitor that yield this value is 10 kΩ and 2.7 nF.

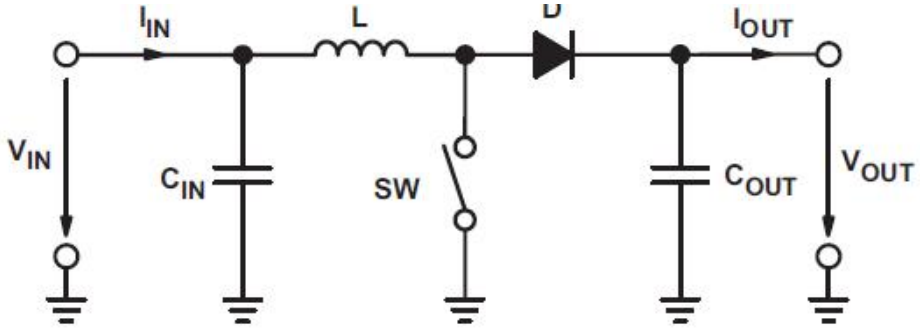

Figure 3: Boost Converter Power Stage

The frequency was deduced from equation 1 of the IC UC3843 data sheet (Compensation *et al*., 2017).

$$f_s = \frac{1.72}{C_T R_T} \qquad 1$$

Considering Figure 3, the relationship between the out and input voltage is expressed in equation 2 (Hasaneen & Mohammed, 2008):

$$\frac{V_o}{V_s} = \frac{1}{1-D} \qquad 2$$

Where, V_o = output voltage, Vs = input voltage or supply voltage and D = duty cycle. The circuit inductance (L) was evaluated from (3)(Roecker, 2022):

$$L = \frac{V_s D}{\Delta I_L F} \qquad 3$$

Where, F = operating frequency and ΔI_L = change in inductor current. The capacitance of the capacitor was predicted using equation 4 (Aika & Agbontaen, 2018):

$$C = \frac{D}{(\Delta V_C / I_o) F} \qquad 4$$

Where, ΔV_C is the change in capacitor voltage. The efficiency η of the boost converter was calculated using equation 5. R_L is the load resistance and R is the inductor resistance.

$$\eta = \frac{1}{1+\frac{R_L}{(1+D)^2 R}} \qquad 5$$

DOI: 10.56892/bima.v8i4B.1201

Boost Circuit Design

The proposed DC – DC boost circuit specification is as follows:

Out Power (P_o) = 65W, input Voltage (V_{in}) = (3.2 V × 3 Lithium-Ion battery) = 9.6 V, output Voltage (V_o) = 20 V, operating Frequency F = 63.7 kHz. The Output Current (I_O) equation is given by equation 6 (Navas, 2018).

$$I_o = \frac{P_o}{V_o} \qquad 6$$

$$I_o = \frac{65}{9.6} = 3.25\ A$$

From equation 2, $D = 1 - \frac{V_{in}}{V_{out}}$

$$D = 1 - \left(\frac{9.6}{20}\right) = 0.53$$

The relationship between the input power (P_{in}), output power (P_O) and power – transfer efficiency is given by (Luo, *et al*., 2010)(Dominic, 2020).

$$\eta = \frac{P_o}{P_{in}}, \qquad 7$$

$$\eta = \frac{I_o V_o}{I_{in} V_{in}}$$

Where, η = Efficiency and I_{in} = Input current. The maximum input current is also the maximum current through the inductor, η was assumed to be 90%.

$$I_{Lmax} = \frac{I_o V_o}{\eta V_{in}} \qquad 8$$

$$=>$$

$$I_{Lmax} = \frac{3.25 \times 20}{0.90 \times 9.6} = 7.52\ A$$

The inductor sizes are chosen such that the change in inductor current is no more than 10 % of the average inductor current.

$$\Delta I_L = 0.1 \times I_{Lmax} \qquad 9$$

Applying 3, the ripple change in the inductor current would require an inductor size of;

$$L = \frac{9.6 \times 0.53}{0.752 \times 63.7kHz} = 107\ \mu H$$

The inductor chosen for this work is closer to this is value = 100 µH. The variation in output voltage is expected to be less than 0.1 x 20 = 2.0. However, a value of 1V was Chosen. Output voltage variation (ΔV_o) = 1V. thus, from equation 4 the capacitance can be found as follows:

$$\boldsymbol{C = \frac{0.53}{\left(1/3.25\right) \times 63.7kHz}} = 27\ \mu F$$

A 33 µF capacitor being closer value was selected. The switch chosen is IRF2807 MOSFET of high IDS current (82A)and low drain source resistance of 13mΩ(Vishay, 2002).The boost circuit was also simulated in Proteus software, based on the calculated parameters. The parameters were the duty cycle, inductor, capacitor, and DC input voltage source.

Rectifier Diode Selection

For loss minimization, Schottky diode was incorporated. Moreover, the forward current value needed is equal to the maximum output current (Hauke*at al*., 2022).

$$I_F = I_{out(max)}$$

Where I_F = average forward current of the rectifier diode, and I_{out}(max) = maximum output current necessary in this work. (International Rectifier, 2010)SB520 Schottky diode have a much higher peak current (5A) rating is therefore chosen.The next parameter that was been checked is the power dissipation of the diode given by equation 10.

$$P_D = I_F \times V_F \qquad 10$$

I_F stands for the average forward current of the rectifier diode and V_F represents forward voltage of the rectifier diode.

Bima Journal of Science and Technology, Vol. 8(4B) Jan, 2025 ISSN: 2536-6041

DOI: 10.56892/bima.v8i4B.1201

Output Voltage Setting

Nearly the output voltage of all conventional converters is with a resistive divider network (which is an integrated part of the design for fixed output voltage converters), the circuit diagram of which is shown in Figure 4. Through the given feedback voltage, V_{FB}, and feedback bias current, I_{FB}, the voltage divider was calculated.

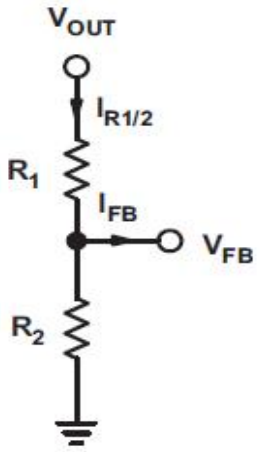

Figure 4: Resistive Divider for Output Voltage Setting

At minimum, 100 times the size of the feedback bias current must be present in the resistive divider as related by equation 11 (Hauke *et al*., 2022.):

$$I_{R1/2} \geq 100 \times I_{FB} \qquad 11$$

I_{FB} = feedback bias current (obtain from IC's data sheet)

The materials used in boost converter construction were listed in Table 2. The circuit diagram prepared with "Proteus software ", is shown in Figure 5.

Deep Discharge and Reverse Voltage Protection Circuit Design

This module is expected to defend the storage battery from being deeply discharge and also protect the system from destruction when battery polarities were interchanged. In this operation a transistor is used as a switch. It switches ON the coil relay when it is in saturated state and OFF if it is unsaturated. A coil relay is used as a circuit breaker to cut OFF the battery supply when it PD has fallen below 8.2V and switch it ON when it is 8.3 V and above. Red and green LEDs were attached to the relay circuit. The red LED is ON when the battery PD is low while the green is ON when the battery's PD is within the normal operation (Martell, 2014). To stop the kickback voltage in the reverse polarity from damaging the transistor while turning ON a relay coil, it is essential to incorporate 1N4001 diode. The materials used in the circuit construction were listed in Table 3.0. The circuit diagram prepared with "Proteus" is illustrated in Figure 6.

Table 2: Lists of Components Used on Boost Converter

S/N	Component	Description	Quantity
1	Resistor	10 kΩ	4
2	Resistor	100 kΩ	1
3	Resistor	10 Ω	1
4	Resistor	1 kΩ	2
4	Variable Resistor	5 kΩ	1
5	Inductor	100 µH	1
6	Capacitor	2.7nF	1
7	Capacitor	1 nF	1
8	Capacitor	10 µF	2
9	Capacitor	47 µF	1
10	Capacitor	33 µF	1
11	Schottky Diode	SB520	1
12	MOSFET	IRF2807	1

Bima Journal of Science and Technology, Vol. 8(4B) Jan, 2025 ISSN: 2536-6041

DOI: 10.56892/bima.v8i4B.1201

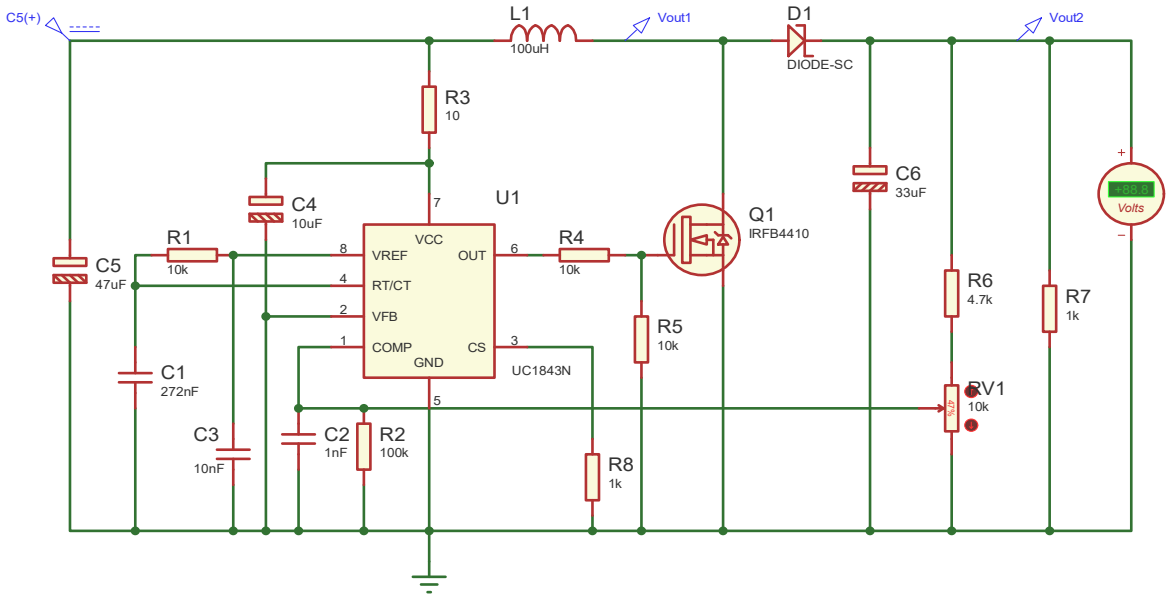

Figure 5: Boost Converter Circuit Design in Proteus

Table: 3.0 Components Used on Protection Circuit

S/N	Component	Description	Quantity
	Resistor	2.2 kΩ	3
	Resistor	1 kΩ	2
	Variable Resistor	20 kΩ	1
	Diode	1N4001	2
	Coil Relay	12 V	1
	LED	Red	1
	LED	Green	1
	Shunt Regulator	TL431	1
	Transistor	2N2905	1

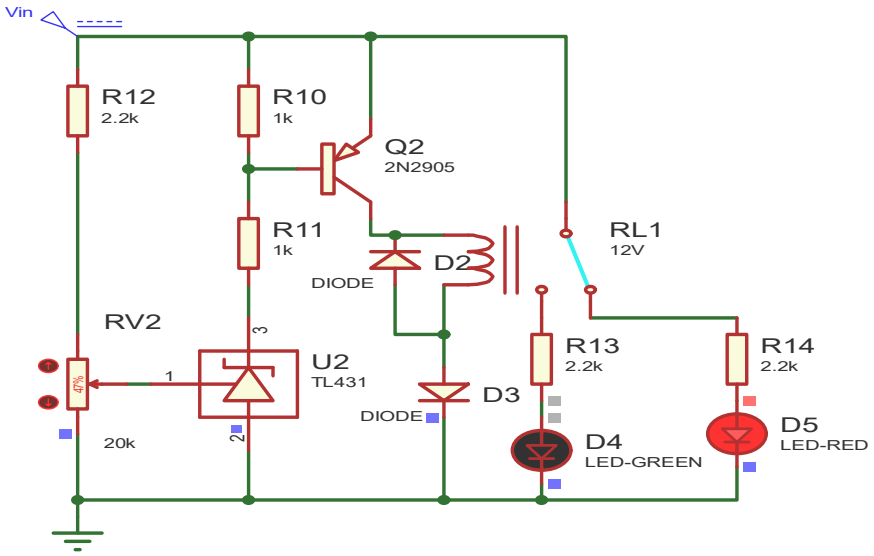

Figure 6: Deep Discharge and Reverse Polarity Protection Circuits Design in Proteus

Bima Journal of Science and Technology, Vol. 8(4B) Jan, 2025 ISSN: 2536-6041

DOI: 10.56892/bima.v8i4B.1201

System Construction

The components were independently verified before soldering,while the Vero board surface was clean to ensure good contact. The two modules (boost converter and the protection circuit) were constructed on a piece of Vero board as shown in Plate 1. Alternative input terminal that bypasses the battery deep discharge protection was provided for connection directly to the solar panel. The photograph of the system is shown in plate 1and plate 2 is the photograph of the system in a plastic casing coupled together with a voltmeter module.

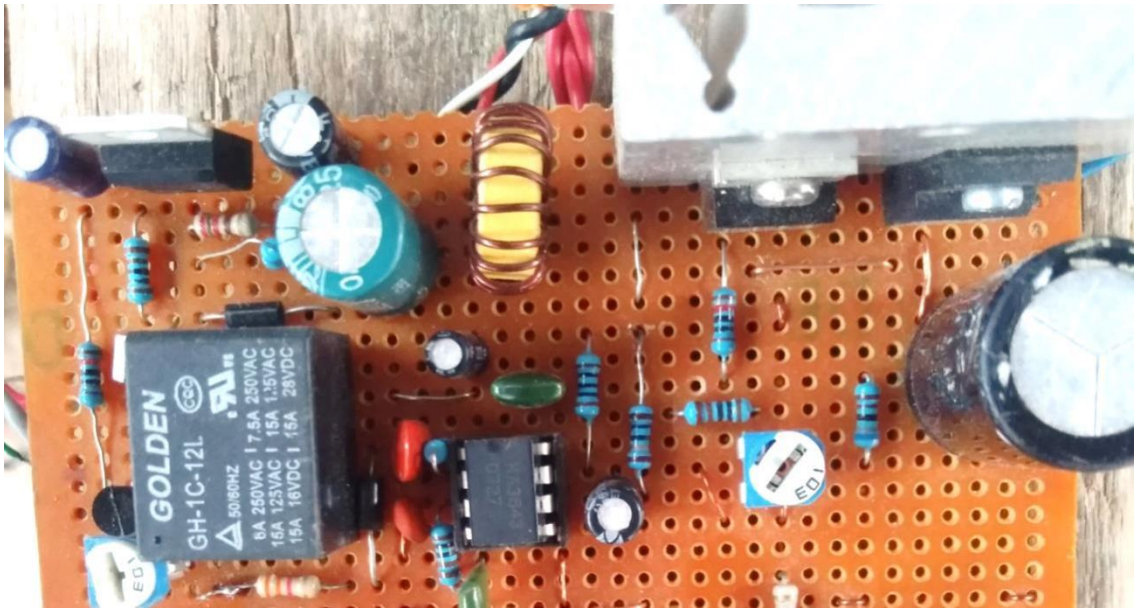

Plate 1: Photograph of the System

Plate 2: Photograph of the System in a plastic casing

DOI: 10.56892/bima.v8i4B.1201

RESULTS AND DISCUSSION

Computer Simulations

After designing the circuit, it was implemented on Proteus software. The control circuit was simulated while input terminals were in the reverse polarity. The result shows that no conduction took place. Simulation test was also carried out with different input voltages and found that the deep discharge protection circuit is working properly. The oscillator wave form was traced via an inductor and found to be a square wave of higher frequency as shown in figure 7.The output PD of the boost converter was found to be a DC supply as shows in Figure 8. The magnitude of the output PD depends on the adjustment of the variable resistor RV1.

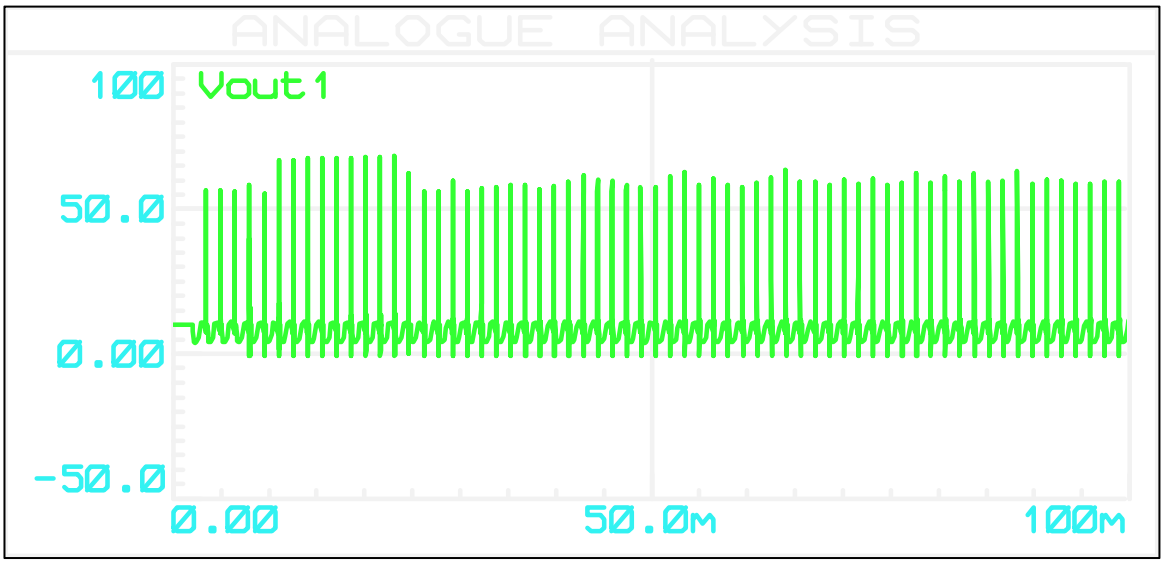

Figure 7: Simulation Test across the Inductor

The simulation shows a square wave at high frequency. Ripple voltage was found to be within the wave at some intervals.

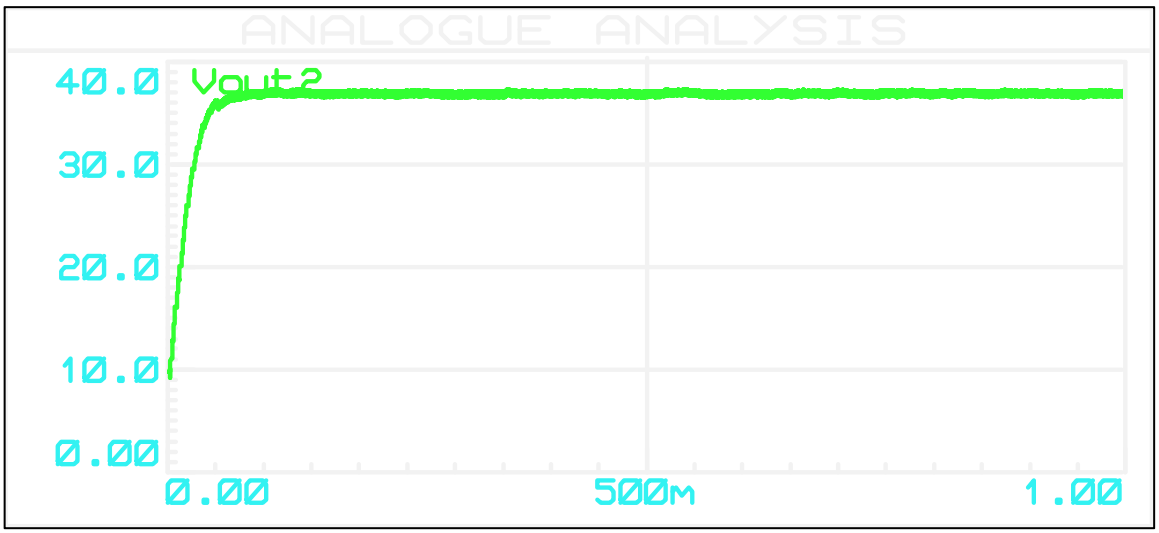

Figure 8: Simulation of the converter output stage in Proteus

Bima Journal of Science and Technology, Vol. 8(4B) Jan, 2025 ISSN: 2536-6041

DOI: 10.56892/bima.v8i4B.1201

System Tests

Test was conducted on the two modules after the completion of the construction exercise. A digital voltmeter was connected across the output of the protection module. The meter shows zero output when the input supply is either in the reverse polarity or lower than 8.2 volt. For low input supply the red LED light is ON. This shows that the module is working as anticipated. The second module was tested by supplying a PD of 8.3 volt and above on a proper polarity. The voltmeter was also connected to the output of the boost converter module. The result shows an output PD greater than that of an input supply. This is an indication that the input PD is being boosted, and found that its magnitude depends on VR1 adjustment. To estimate the power delivered by the system, a non-inductive/capacitive load was connected across it output. A variable load resistance (high power rheostat) connected across was then varied between5 - 8 Ω. Potential differences were measured in accordance to resistances across. Results obtained were represented graphically in Figure 9. The result shows that the circuit can deliver a peak power of around, $P = \frac{V^2}{R} = \frac{20\times20}{6.3} = 64.5\ watts$. While the projected power was 65 watts and 90 % efficiency, the overall efficiency after implementation was found to be 89 %.

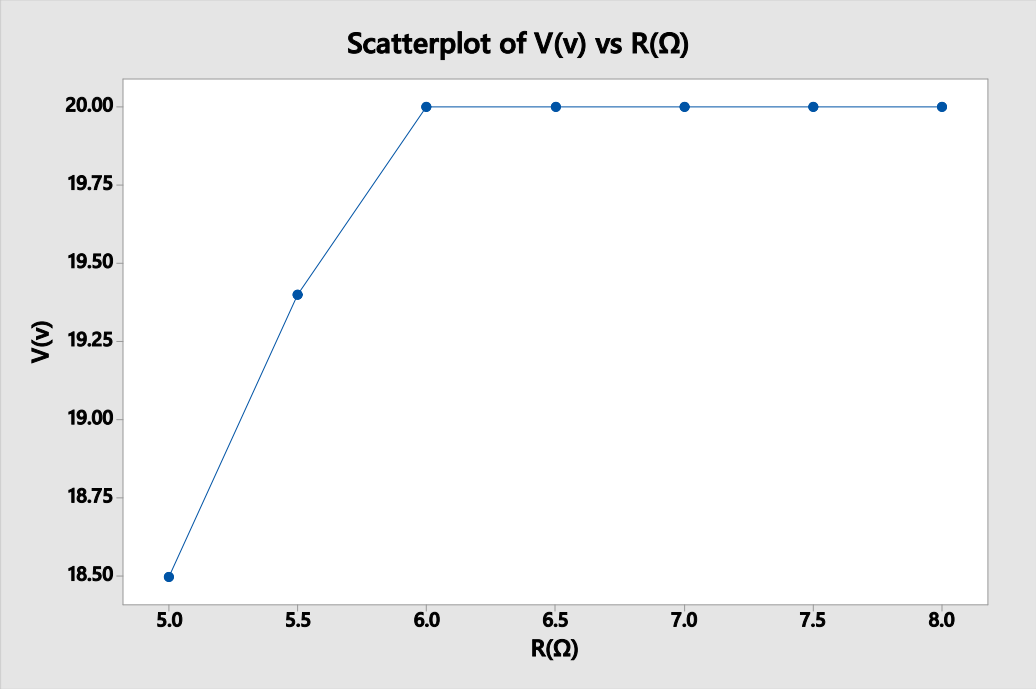

Figure 9: Plot of V against R

CONCLUSION

The designed and implemented laptop power bank, operates on an inbuilt storage battery of PD 9.6 volt and gives an output PD 12 to 20 volts that is suitable for charging most of the laptops within the locality. The storage battery can be recharge via mains supply or solar panel. It can deliver an output power of 64.5 watts and 89% efficiency. It was tested with different laptops including mini systems that operates on 12 volt PD and found to be working satisfactory. For future improvement in the functionality, efficiency and usability, it

DOI: 10.56892/bima.v8i4B.1201

is recommended that a load-sharing circuit be added to allow the power bank to charge devices while simultaneously being charged. Furthermore, a fast charging technology can be integrated, thus ICs like the IP2716 or TPS25740 can be added to enable fast charging. Lastly, low-power components can be used to minimize energy loss and improve overall efficiency.

acknowledgement

The authors wish to express their appreciation to the Tertiary Education Trust Fund (TETFUND) for Research Funding to Federal University Gusau under the Institutional Based Research (IBR) Scheme with the following subheading
TETF/DR&S/CE/UNIV/GUSAU/IBR/2023/VOL.1

REFERENCES

A. Dominic Savio, A. V. J. (2020). Development of multiple plug-in electric vehicle mobile charging station using bidirectional converter. *International Journal of Power Electronics and Drive System (IJPEDS)*, *11*(2), 785–791.

Aika, T. A., & Agbontaen, F. O. (2018). *DESIGN AND SIMULATION OF A DC – DC BOOST CONVERTER*. 1–8. https://doi.org/10.1109/ISCAS.2006.1692714

Akankpo, A. O., Adeniran, A. O., Ayedun, F., Anyanor, O. O., & Ebong, G. (2023). Development and Construction of Portable Solar Power Packs for Laptops and Small Devices. *Journal of Research in Environmental and Earth Sciences*, *9*(1), 5–63.

Almutairi, A., Sayed, K., Albagami, N., Abo-Khalil, A. G., & Saleeb, H. (2021). Multi-port pwm dc-dc power converter for renewable energy applications. *Energies*, *14*(12), 3490.

B. Yang, W. Li, Y. Zhao, and X. H. (2010). Design and analysis of a Grid connected photovoltaic power system. In *IEEE Trans. Power Electron., vol. 25,no. 4,* (pp. 992–1000).

Baby, T. (2015). *Boost Converter*. Gyeongsang National University. https://doi.org/DOI:10.13140/RG.2.2.31386.95687

Compensation, A. F., Limiting, P. C., Characteristics, E. L., Lockout, U., Hysteresis, W., Suppression, D., Output, H. T., Trimmed, I., Reference, B., Amplifier, E., Low, W., & Resistance, O. (2017). *UCx84x Current-Mode PWM Controllers*.

Czerniak, J., Gacek, A., & Szopa, P. (2021). Analysis of Power Bank Quality Criteria That Are Important from the Consumer's Point of View. *Energies*, *14*(18), 5747.

D'Amico, Mar´ıa Bel´en; Oliva, Alejandro; Paolini, Eduardo; Guerin, N. (2006). Bifurcation Control of a Buck Converter in Discontinuous Conduction Mode. In *IFAC Proceedings Volumes 39(8)* (pp. 389–394). 39(8). https://doi.org/doi:10.3182/20060628-3-FR-3903.00069

Edison, Banguero Correcher, AntonioPérez-Navarro A, Morant F, Aristizábal Cardona, A. J. (2018). *A Review on Battery Charging Control Strategies: Application to Renewable Energy Systems*. *11*. https://doi.org/DOI 10.3390/en11041021, Energies Journal

Ezzitouni, J., Ahmed, M., Mohammed, L., & Ayoub, K. (2021). *Management of battery charging and discharging in a photovoltaic system with variable power demand using artificial neural networks*. *01037*, 2–6.

Ghavipanjeh Marangalu, M., Vosoughi Kurdkandi, N., & Babaei, E. (2021).

DOI: 10.56892/bima.v8i4B.1201

Single-source multilevel inverter based on flyback DC-DC converter. *IET Power Electronics*, *14*(7), 1237–1255. https://doi.org/https://doi.org/10.1049/pel2.12101

Hasaneen, B. M., & Mohammed, A. A. E. (2008). *DESIGN AND SIMULATION OF DC / DC BOOST CONVERTER*. 335–340.

Hauke, B., Power, L., & Dc, D. C. (n.d.). *Basic Calculation of a Boost Converter ' s Power Stage*. *November 2022*, 1–10.

International Rectifier. (2010). *IRF2807PbF IRF2807PbF* (pp. 1–9). International Rectifier.

Kuncoro, C., Asyikin, M. B. Z., & Adristi, C. (2023). Dual mode portable power bank for extending battery life of gadget devices. *AIP Conference Proceedings*, *2665*(1).

Lopa, S. A., Hossain, S., Hasan, M. K., & Chakraborty, T. K. (2016). *Design and Simulation of DC-DC Converters Design and Simulation of DC-DC Converters*. *January*.

Luo, F. L, Ye H., and Rashid, M. H. (2010). *Digital Power Electronics and Applications* (p. 7). Elsevier Publisher.

Martell, M. (2014). *Transistor as a switch*. Transistor as a Switch, Using Bipolar Transistor as Switches.

Navas, K. A. (2018). PHI Learning Pvt. Ltd. In *Electronics Lab Manual (Volume 2)* (p. 288). PHI Learning Pvt. Ltd.

Norum, F. S. and L. (2010). 36th Annual Conference on IEEE Industrial Electronics Society. *Effective Use of Fifilm Capacitors in Single-Phase Pv-Inverters by Active Power Decoupling*, 2784 –2789.

Prochazka Petr, Cervinka Dalibor, Martis Jan, Cipin Radoslav, Vorel, P. (2016). Li-Ion Battery Deep Discharge Degradation. *ECS Transistor*, *74*, 31–36. https://doi.org/DOI 10.1149/07401.0031esct

Roecker, G. (2022). *How to Design a Boost Converter Using the LM5156*. *June 2020*.

Sedaghati, F., & Pourjafar, S. (2020). Analysis and implementation of a boost DC–DC converter with high voltage gain and continuous input current. *IET Power Electronics*, *13*(4), 798–807.

Shukla, A., Jain, P., Gupta, D., Tejas, Y. V., Chaudhary, R., & Tyagi, S. (2024). Versatile empowering of smart devices using proposed power banks and chargers: Study, review and comparison analysis. In *Artificial Intelligence and Information Technologies* (pp. 177–181). CRC Press.

Vishay. (2002). *SB520 thru SB560 Vishay General Semiconductor TYPICAL APPLICATIONS PRIMARY CHARACTERISTICS SYMBOL SB520 thru SB560* (Issue 1, pp. 1–4). Vishay USA.